



Dynamics of T Cell-Mediated Immune Signaling Network During Pathogenesis of Chronic Obstructive Pulmonary Disease

Chae Min Lee^{1,2*}, Andrew Sehoon Kim^{3*}, Minki Kim^{1,2}, Jae Woong Jeong⁴,
Sugyeong Jo^{1,2}, Nahee Hwang², and Sungsoo Fang^{1,2,5}

¹Graduate School of Medical Science, Brain Korea 21 Project, Yonsei University College of Medicine, Seoul, Korea;

²Department of Biomedical Sciences, Gangnam Severance Hospital, Yonsei University College of Medicine, Seoul, Korea;

³Department of Neuroscience, Vanderbilt University College of Arts and Science, Vanderbilt University, Nashville, USA;

⁴Department of Medicine, Yonsei University College of Medicine, Seoul, Korea;

⁵Chronic Intractable Disease for Systems Medicine Research Center, Yonsei University College of Medicine, Seoul, Korea.

Purpose: Chronic obstructive pulmonary disease (COPD) is characterized by alveolar destruction and increased inflammation, leading to respiratory symptoms. This study aimed to identify the traits for COPD progression from mild to severe stages. Additionally, we explored the correlation between coronavirus disease-2019 (COVID-19) and COPD to uncover overlapping respiratory patterns.

Materials and Methods: Bulk RNA sequencing was conducted on data from 43 healthy individuals and 39 COPD patients across one dataset (GSE239897) to distinguish COPD characteristics. Single-cell RNA analysis was then performed on samples from seven mild patients, seven moderate patients, and three severe patients from three datasets (GSE167295, GSE173896, and GSE227691) to analyze disease progression. Finally, single-nuclei RNA analysis was applied to data from seven healthy individuals and 20 COVID-19 patients from one dataset (GSE171524) to compare the two conditions.

Results: Bulk RNA sequencing revealed enhanced inflammatory pathways in COPD patients, indicating increased inflammation. Single-cell RNA sequencing showed a stronger inflammatory response from mild to moderate COPD with a decrease from moderate to severe stages. COVID-19 displayed similar biological patterns to moderate COPD, suggesting that stage-specific COPD analysis could enhance COVID-19 management.

Conclusion: The analysis found that immune responses increased from mild to moderate stages but declined in severe cases, marked by reduced pulmonary T cell activation. The overlap between moderate COPD and COVID-19 suggests shared therapeutic strategies, warranting further investigation.

Key Words: Chronic obstructive pulmonary disease, COVID-19, single-cell RNA sequencing

Received: August 2, 2024 **Revised:** November 5, 2024

Accepted: November 6, 2024 **Published online:** February 14, 2025

Corresponding author: Sungsoo Fang, PhD, Department of Biomedical Sciences, Yonsei University College of Medicine, 50-1 Yonsei-ro, Seodaemun-gu, Seoul 03722, Korea.
E-mail: sfang@yuhs.ac

*Chae Min Lee and Andrew Sehoon Kim contributed equally to this work.

•The authors have no potential conflicts of interest to disclose.

© Copyright: Yonsei University College of Medicine 2025

This is an Open Access article distributed under the terms of the Creative Commons Attribution Non-Commercial License (<https://creativecommons.org/licenses/by-nc/4.0>) which permits unrestricted non-commercial use, distribution, and reproduction in any medium, provided the original work is properly cited.

INTRODUCTION

Despite significant advancements in medicine over recent decades, factors such as smoking, air pollution, and aging have contributed to a sharp increase in the number of patients with respiratory problems worldwide.^{1,2} In particular, chronic obstructive pulmonary disease (COPD) has been on the rise.³ In 2019, COPD was responsible for 3.23 million deaths, becoming the third leading cause of death.⁴ Given its impact, the relevance of this disorder has led to increased interest in identifying the biological mechanisms and ways to mitigate this condition.

Current research primarily attributes immune dysfunction, particularly T cell activation, to the development and progression of COPD.

While initial research has explored COPD's immunopathology, the specific mechanisms driving the progression between different stages of the disease, as defined by the Global Initiative for Chronic Obstructive Lung Disease (GOLD) criteria, is still relatively unknown. Identifying biomarkers that indicate COPD progression is critical for potential treatment and early prevention.

In this study, we grouped patients into three categories—mild, moderate, and severe—based on the GOLD criteria, which evaluates forced expiratory volume in one second (FEV1%) to measure disease severity. Bulk RNA sequencing confirmed higher inflammation and T cell activation in COPD patients compared to age-matched controls, while single-cell RNA sequencing (scRNA-seq) revealed distinct biological differences between the stages, suggesting significant shifts in underlying pathways. These findings highlight the importance of addressing COPD progression based on stage-specific biological changes.

Moreover, the coronavirus disease-2019 (COVID-19) pandemic has strongly emphasized the need for research into interactions between COPD and other respiratory diseases. Patients with COPD have weakened immune responses and are more susceptible to severe acute respiratory syndrome coronavirus 2 (SARS-CoV-2). Moreover, T cell dysfunction in COPD exacerbates the severity of both COPD and COVID-19 symptoms. Our findings suggest that the progression of COPD mirrors the pathogenesis of COVID-19, especially in moderate COPD stages. This highlights the need for stage-specific research in both conditions.

MATERIALS AND METHODS

Comparison of bulk RNA sequencing in COPD patients and controls

Publicly available dataset GSE239897 from the Gene Expression Omnibus (<https://www.ncbi.nlm.nih.gov/geo/>) were accessed to perform bulk RNA sequencing analysis of lung tissue. Data from GSE239897 included 43 age-matched control samples and 39 COPD samples.

The “GSEA” software (version 4.3.2) facilitated the generation of Gene Set Enrichment Analysis (GSEA) data. For each dataset, we created and loaded gct and cls files into the program. The Hallmark Gene Sets database (h.all.v2023.2.Hs.symbols.gmt) was referenced. The number of permutations was set to 1000, with gene symbols collapsed and the permutation type based on phenotype. The chip platform selected was “Human_Gene_Symbol_with_Remapping_MsigDB.v2023.2.Hs.chip.”

Additionally, to evaluate the expression of each gene, we utilized files containing Fragment Per Kilobase of transcript per

Million mapped reads (FPKM) values provided by each dataset. Gene expression values were extracted from these files and visualized using “GraphPad Prism” (version 9.5.1).

Acquisition of scRNA-seq data

scRNA-seq data from lung tissues of 17 patients were collected from the datasets GSE227691, GSE173896, and GSE167295. The data were categorized into four groups based on the GOLD criteria. The groups were divided by using FEV1. Patients with mild COPD had a FEV1% of 80% or higher, moderate patients had a FEV1% between 50% and 79%, severe patients had a FEV1% between 30% and 49%, and very severe patients had a FEV1% below 30%. Due to limited number of individuals in the very severe category, the categories for severe and very severe were combined into one, resulting in seven mild COPD patients, seven moderate COPD patients, and three severe COPD patients. The exact FEV1% and supplementary patient information are provided in Table 1.

scRNA-seq data processing

For initial quality control (QC) and downstream analyses, Seurat (version 4.3.1) package was used in R. First, all data from 17 patients were loaded into R through the Read10X function, then converted into a Seurat object. Next, QC was performed to remove any low-quality cells depending on three factors: num-

Table 1. Information and Classification of COPD scRNA-seq Data

Identification	FEV1%	Age	Gender	Dataset	Labeling
Mild					
Mild 1	97.3	52	M	GSE227691	GSM7105665
Mild 2	112.7	76	M	GSE227691	GSM7105666
Mild 3	92.9	67	M	GSE227691	GSM7105667
Mild 4	109.4	61	M	GSE227691	GSM7105668
Mild 5	102.0	70s	F	GSE173896	JK05
Mild 6	82.6	80s	M	GSE173896	JK07
Mild 7	88.7	80s	M	GSE173896	JK08
Moderate					
Moderate 1	78.7	70	M	GSE227691	GSM7105669
Moderate 2	62.6	80	M	GSE227691	GSM7105670
Moderate 3	70.5	61	M	GSE227691	GSM7105671
Moderate 4	76.8	78	M	GSE227691	GSM7105672
Moderate 5	79.6	60s	M	GSE173896	JK02
Moderate 6	77.1	70s	M	GSE173896	JK09
Moderate 7	74.6	80s	M	GSE173896	JK10
Severe					
Severe 1	33.0	65	F	GSE167295	100998
Very severe					
Severe 2	22.0	62	F	GSE167295	100999
Severe 3	21.0	61	F	GSE167295	101000

COPD, chronic obstructive pulmonary disease; scRNA-seq, single-cell RNA sequencing; FEV1%, forced expiratory volume in one second. Detailed information is provided for a total of 17 COPD patients from GSE227691, 173896, and 167295.

ber of genes detected per cell (nFeature), total molecule counts per cell (nCOUNT), and percentage of mitochondrial genes (percent_MT). The values for which these factors were adjusted are listed in Supplementary Table 1 (only online). After QC, each Seurat object was imputed using the “RunALRA” function, then normalized with the “LogNormalize” function and multiplied by a default factor of 10000. The most variable genes within the objects were identified using the “FindVariableFeatures” function. Lastly, integration was performed using the “IntegrateData” function.

For easier visualization and analysis, principal component analysis (PCA) was performed using R. The “RunPCA” function was utilized to create a Uniform Manifold Approximation and Projection (UMAP) with 30 significant principal components. Subsequently, the “FindNeighbors” function created a shared nearest-neighbor graph, while “FindClusters” identified relevant clusters by refining shared nearest-neighbor modularity. The representative genes of clusters were found using “FindAllMarkers” based on those with a log fold change greater than 0.25. Cluster annotation was accomplished by a two-step verification process using the singleR package and PanglaoDB (<https://panglaoDB.se/search.html>), a database for marker genes verified from multiple studies. The singleR package from Bioconductor allowed automatic annotation, and the verified representative marker genes were compared to those from PanglaoDB.

Cell-cell communication analysis

Cell-to-cell communication analysis was conducted on a total of 12 cell types using the R package “CellChat” (version 1.6.1). To visualize the signaling activity of T cells, the “netVisual_circle” function was used. Subsequently, the multiple dataset comparison analysis function was used to analyze the interactions between mild and moderate (MM) cases, as well as between moderate and severe (MS) cases. The “netVisual_heatmap” function was then used to visualize a heatmap showing the variation in the number of interactions or the strength of interactions among various cell populations across the two datasets. Additionally, the “rankNet” function was applied to confirm the relative information flow. To obtain results for when T cells acted as targets and sources, the supplementary parameters “targets.use” and “sources.use” were utilized.

GSEA based on differentially expressed genes

Subsets for mild vs. moderate and moderate vs. severe were created by applying the “subset” function on each pair of types within a single dataset. Differentially expressed genes (DEGs) were then extracted from the clusters based on MS expression using the “FindMarkers” function. Subsequently, GSEA analysis was performed using the R package “clusterProfiler” (version 4.10.0). To compare the expression levels of genes associated with each pathway, we used the average log2 fold change and -log10 adjusted *p*-values obtained from the “FindMark-

ers” function. These values were visualized using the “ggplot2” package.

Collection of single-nuclei RNA sequencing data from COVID-19 patients

Single-nuclei RNA sequencing (snRNA-seq) data of lung tissues from seven control individuals and 20 COVID-19 patients were sourced from GSE171524. Specific patient information is provided in Table 2. The preprocessed data was imported and converted into a Seurat object using the “CreateSeuratObject” function.⁵ Following this, the data was normalized using the “NormalizeData” function, and the most variable genes were identified with the “FindVariableFeatures” function. Then, the “ScaleData” and “RunPCA” functions were applied. Finally, the

Table 2. Information Regarding COVID-19 Patient Data

Identification	Age	Gender	Interval death symptoms onset days	Intubation days	Lung pathology
Control					
C51ctr	70	F	-	-	-
C52ctr	69	F	-	-	-
C53ctr	79	M	-	-	-
C54ctr	72	F	-	-	-
C55ctr	69	M	-	-	-
C56ctr	75	M	-	-	-
C57ctr	68	M	-	-	-
COVID-19					
L01cov	70	M	<4	1	COVID, congestion
L03cov	73	M	16	0	COVID, DAD
L04cov	NA	F	11	0	COVID, DAD
L04covaddon	NA	F	11	0	COVID, DAD
L05cov	78	F	28	12	COVID, DAD
L06cov	80	F	22	0	COVID, DAD
L07cov	80	M	>28	NA	COVID, DAD
L08cov	83	M	10	0	COVID, DAD
L09cov	79	M	15	0	COVID, DAD
L10cov	84	M	NA	10	COVID, DAD
L11cov	71	M	27	1	COVID, DAD
L12cov	80	F	27	25	COVID, DAD
L13cov	63	M	28	9	COVID, DAD
L15cov	68	M	28	20	COVID, DAD
L16cov	70	F	50	41	COVID, DAD
L17cov	65	M	25	7	COVID, DAD
L18cov	72	M	54	45	COVID, DAD
L19cov	69	F	>40	0	COVID, congestion
L21cov	68	F	45	36	COVID, DAD
L22cov	58	M	63	56	COVID, congestion

DAD, diffuse alveolar damage.

The table provides comprehensive details for both control individuals and COVID-19 patients obtained from the GSE171524.

“RunUMAP” function was executed with reduction set to PCA and dimensions 1:30, followed by the “FindNeighbors” function. Clustering was performed using “FindClusters” with a resolution parameter of 1.5. The annotations provided by the authors were adhered to during the analysis. T cell subsetting was performed using the “subset” function, and DEGs were identified using the “FindMarkers” function. Additionally, the “clusterProfiler” package was employed for GSEA. The “VlnPlot” function was used to create violin plots, and statistical analyses were performed using the “stat_compare_means” function from the “ggpubr” package.

RESULTS

COPD patients exhibited strong expression of inflammatory and T cell-related signatures

To investigate differences in the expression levels of inflammation and T cell-related genes between COPD patients and age-matched controls, bulk RNA sequencing analysis was conducted using the GSE239897 dataset (Fig. 1A). GSE239897 comprised data from 43 controls and 39 COPD patients. We used GSEA to compare controls and COPD samples at the MSigDB Hallmark Gene Sets level in order to gain insight into the characteristics of COPD. We confirmed a significant enrichment of inflammatory response, interferon (IFN)- γ response, and tumor necrosis factor-alpha (TNF- α) signaling via nuclear factor-kappa B (NF- κ B) in COPD across the cohort (Fig. 1B).

Then, we assessed the expression of genes associated with

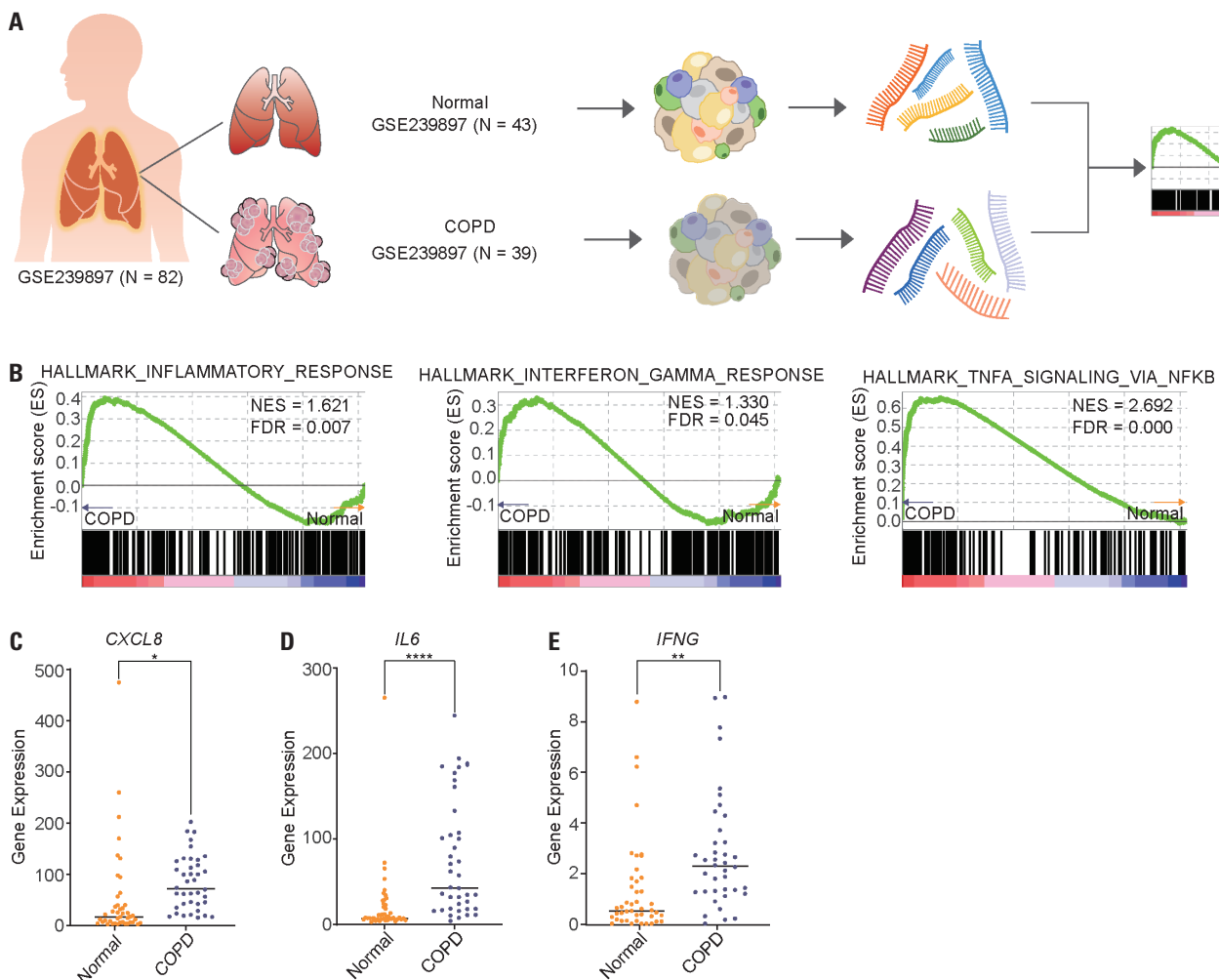


Fig. 1. COPD prominently exhibiting inflammation and T cell activation. (A) The experimental design for bulk RNA sequencing involved dataset from control subjects (n=43) and COPD patients (n=39). The dataset was acquired from GSE239897. (B) Enrichment plots depict the enrichment scores of the inflammatory response, interferon gamma response, and TNF- α signaling via NF- κ B from the hallmark dataset. In all plots, COPD exhibits a higher score compared to control individuals. (C and D) Dot plot displaying the gene expression levels of control and COPD patient data. Both CXCL8 and IL6 gene expressions, associated with inflammation, are higher in COPD patients. (E) Dot plot illustrates the gene expression levels of control and COPD patient data. The expression of IFNG gene, associated with T cell activation, is elevated in COPD patients (* $p < 0.1$, ** $p < 0.01$, **** $p < 0.0001$). COPD, chronic obstructive pulmonary disease; NES, normalized enrichment score; FDR, false discovery rate; TNF- α , tumor necrosis factor-alpha; NF- κ B, nuclear factor-kappa B.

inflammation in the dataset of each patient group for a more detailed comparison between the control group and COPD patients. Upon examining the expression levels of the CXCL8 gene, well-known for its association with inflammation, the average expression level was higher in COPD patients compared to control individuals (Fig. 1C).⁶ Despite the presence of control data slightly deviating in the cohort, the overall expression level was lower compared to COPD patients. Additionally, we compared IL6, another inflammation-related gene.⁷ IL6 showed a similar trend to CXCL8 (Fig. 1D). Dataset exhibited outlier values, indicating that not all data consistently fall within high or low ranges; however, the average value was significantly lower in control individuals compared to COPD patients overall. This showed that COPD patients exhibited a stronger inflammatory phenomenon. Considering the critical role of T cells in COPD, we proceeded to compare the expression of genes associated with T cells. We examined the expression levels of the IFN- γ gene, a marker for T cell activation.⁸ Notably higher expression was observed in COPD compared to controls in GSE239897 (Fig. 1E). Thus, it is evident that T cell activation significantly increases in COPD conditions. Overall, our data highlights pronounced phenomena related to inflammation and T cell activation in COPD compared to controls.

Single-cell analysis revealed that T cell populations increased as COPD progressed

To investigate the changes occurring as COPD progresses, we initially conducted scRNA-seq analysis on lung tissues from patients classified as mild, moderate, and severe (Fig. 2A). A total of three datasets, namely GSE227691, GSE173896, and GSE167295, were used (Table 1). Through this analysis, various categories of cell types were identified, including natural killer cells (GNLY, FGFBP2), T cells (CD3D, CD3G), macrophages (CD68, CD163), endothelial cells (PECAM1, CD93), pulmonary alveolar type I (Pul1/AGER, PDPN), pulmonary alveolar type II (LAMP3, SFTPC), fibroblasts (COL1A1, PDGFRA), mast cells (TPSAB1, HDC), B cells (CD19, MS4A1), ciliated cells (CCDC17, CCDC39), Clara cells (SCGB1A1, BPIFA1), and pericytes (ACTA2, DES) (Fig. 2B and Supplementary Fig. 1A, only online).⁹⁻²⁰ Subsequently, these cell types were annotated using representative marker genes (Fig. 2C and Supplementary Fig. 1B, only online). A total of 55154 cells were analyzed, derived from seven mild patients, seven moderate patients, and three severe patients. Upon specific investigation of cell proportions at each stage, heterogeneous patterns emerged (Fig. 2D). Particularly, a trend was observed where the proportion of T cells decreased slightly from the mild to moderate stages, before increasing again as the disease progressed to severe (Fig. 2E). Accordingly, the exploration of interactions between clusters revealed a decrease in interactions involving T cells in the severe stage (Fig. 2F). Thus, as COPD patients advanced to the severe stage, an increase in T cell proportion was accompanied by reduced interactions with neighboring

cell clusters.

MM and MS exhibited different aspects of interactions

Prior to analyzing interactions between cell clusters, we designated the comparison between MM, and the comparison between MS. Initially, the interaction counts and interaction strength between MM and MS were compared. When focusing on T cells, it can be observed that the number of interactions in MM increased slightly when sending and receiving (Fig. 3A). Additionally, the interaction strength showed a similar trend, with MM being almost comparable or slightly increased in moderate. Examining the trends of other cell clusters besides T cells revealed that, except for cases where Pul1 was the sender, most showed a minor increase in interaction count when comparing MM. Furthermore, with the exception of cases where Pul1 was the sender and T cell was the receiver, interaction strength generally increased in moderate compared to mild.

In MS, when comparing MS, both the number of interactions and interaction strength showed an overall decreasing pattern (Fig. 3B). Nonetheless, sporadic instances of increased interaction count or strength were noted. Notably, when T cells functioned as receivers, there was a discernible augmentation in interactions originating from Pul1. Moreover, an elevation in interaction strength between endothelial cells and Pul1 was observed. Conversely, in most comparisons with moderate cases, interactions involving T cells or their associated interaction strength exhibited a marginal decrease in severity.

Additionally, we identified changes in signaling pathways based on the information flow in both comparisons of MM and MS. The two bar graphs illustrate the ranking of significant signaling pathways based on differences in information flow inferred from the network between T cell of MM (Fig. 3C). The left side shows the pathways received by T cells when targeted by other clusters, while the right side shows the pathways T cells sent to other cell clusters. Signaling pathways marked in red indicate those that were significantly stronger in mild conditions. Pathways shown in black are those that were strong in one condition but did not exhibit a significant *p*-value. Green pathways signify those that were significantly stronger in moderate conditions. It could be observed that, whether T cells were the target or the source, the pathways were stronger in moderate conditions. Additionally, different trends were noted in the two scenarios. Conversely, the right bar graph shows that moderate conditions exhibited a wider variety of signaling pathways compared to severe conditions (Fig. 3D). Here, green indicates pathways with significant *p*-values in moderate conditions, blue indicates pathways that were significantly stronger in severe conditions, and black denotes non-significant pathways.

In summary, both MM and MS exhibited distinct trends when T cells received or emitted signals from other clusters. Particularly, most pathways were prominently expressed in the moderate stage, yet TRAIL and IL10 showed stronger expression when T cells acted as targets in both mild and severe stages.

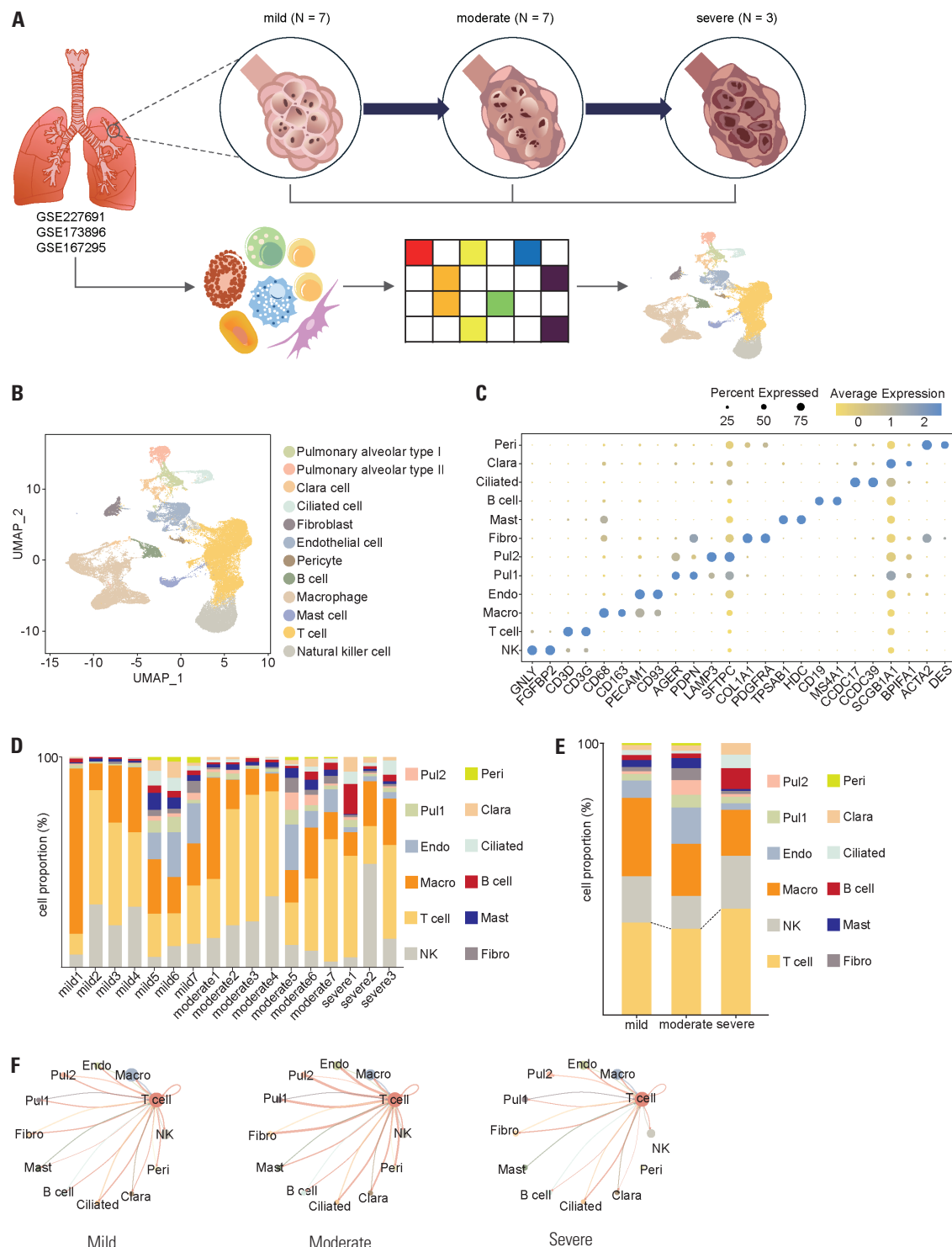


Fig. 2 A change in the trend of T cell behaviors as COPD progresses. (A) Schematic diagram depicts the workflow of single-cell RNA sequencing. Data from seven mild patients, seven moderate patients, and three severe patients were employed in the analysis. The datasets were obtained from GSE227691, GSE173896, and GSE167295. (B) UMAP plot displays 12 integrated clusters with 55154 cells. (C) Dot plot illustrates marker genes used for annotating the twelve clusters in (B). The dot size corresponds to the percentage of cells expressing the marker, while the color scale indicates the average marker expression across all clusters in COPD patients in (A). (D) Bar graphs show the cell proportions for each patient, indicating the heterogeneous nature across all patients. (E) Bar graphs present the overall cell proportions when patient data is combined into mild, moderate, and severe categories. They show a decrease in the proportion of T cells from mild to moderate, followed by an increase towards severe. (F) Circle plots feature the cell-cell communication network between T cells and adjacent cell clusters at each stage of COPD. They demonstrate an increase in interactions from mild to moderate, but a decrease towards severe. COPD, chronic obstructive pulmonary disease; UMAP, Uniform Manifold Approximation and Projection; NK, natural killer cell; Macro, macrophage; Endo, endothelial cell; Pul1, pulmonary alveolar type I; Pul2, pulmonary alveolar type II; Fibro, fibroblast; Mast, mast cell; Ciliated, ciliated cell; Clara, clara cell; Peri, pericyte.

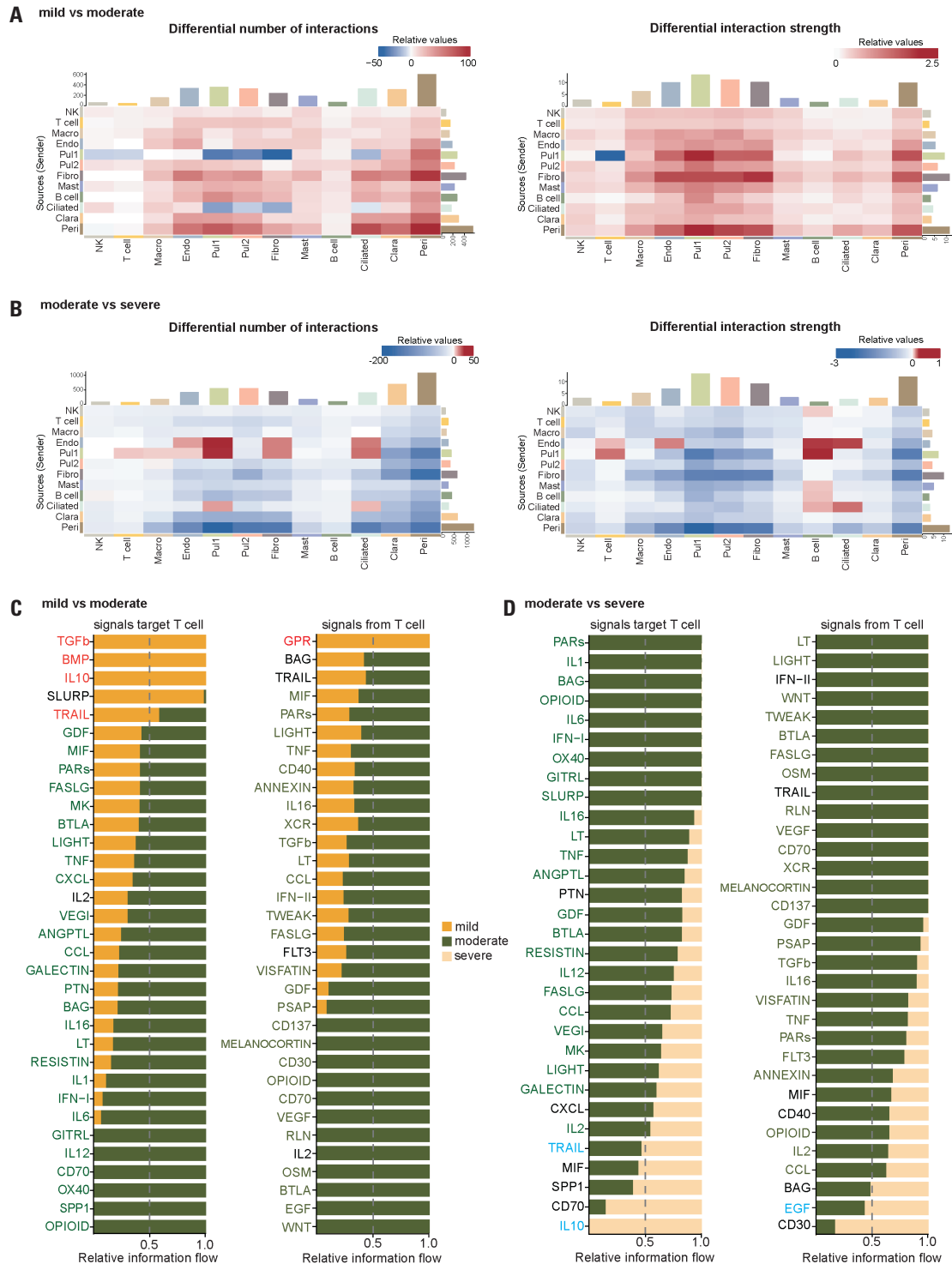


Fig. 3. Changes in relationship with neighboring clusters as COPD progresses to severe. (A) Heatmap illustrates the variance in the number of interactions (left) and interaction strength (right) among distinct cell populations in mild and moderate patients. (B) Heatmap depicts the differential number of interactions (left) and interaction strength (right) in moderate and severe patients. (C) Bar graphs compare the information flow for each signaling pathway between mild and moderate patients. It highlights the differences in signal trends when T cells function as targets versus sources. This flow is defined as the sum of communication probabilities between T cells acting as targets (left) or sources (right) and surrounding cells. Pathways depicted in red exhibit significantly stronger values in the mild, while those in green show significantly stronger values in the moderate. Pathways marked in black denote non-significant p -values. (D) Bar graphs depict the relative information flow between T cells as targets (left) or sources (right) and adjacent cells in moderate and severe patients. Pathways represented in green signify significantly stronger values in the moderate stage, while those in blue signify stronger values in severe patients. Black indicates non-significant p -values. COPD, chronic obstructive pulmonary disease; NK, natural killer cell; Macro, macrophage; Endo, endothelial cell; Pul1, pulmonary alveolar type I; Pul2, pulmonary alveolar type II; Fibro, fibroblast; Mast, mast cell; Ciliated, ciliated cell; Clara, clara cell; Peri, pericyte.

Moreover, when T cells emitted signals, GPR was more strongly expressed in the mild stage, while EGF signal was more pronounced in the severe stage.

Pathway variances in T cell profiles between MM and MS

To specifically examine the changes occurring in T cells, we narrowed down our analysis to pathways expressed in T cells to observe the differences. The normalized enrichment score was calculated based on the upregulated DEGs in both MM and MS datasets to compare the expressed pathways. The comparison

of MM in T cells revealed that the pathways associated with immune responses, such as immunoglobulin production and antimicrobial humoral response, are predominantly highlighted in orange at the top (Fig. 4A). The data suggested that immune response is more pronounced in moderate COPD T cell populations. Moreover, upon comparing the mean expression levels of key genes associated with immune response pathways, such as IL5, LTF, PLA2G1B, TF, and TRAV2, it was evident that they exhibited the highest expression levels during the moderate stage compared to mild and severe stages (Fig. 4B). To verify these findings, we used the average log2 fold change and -log10 ad-

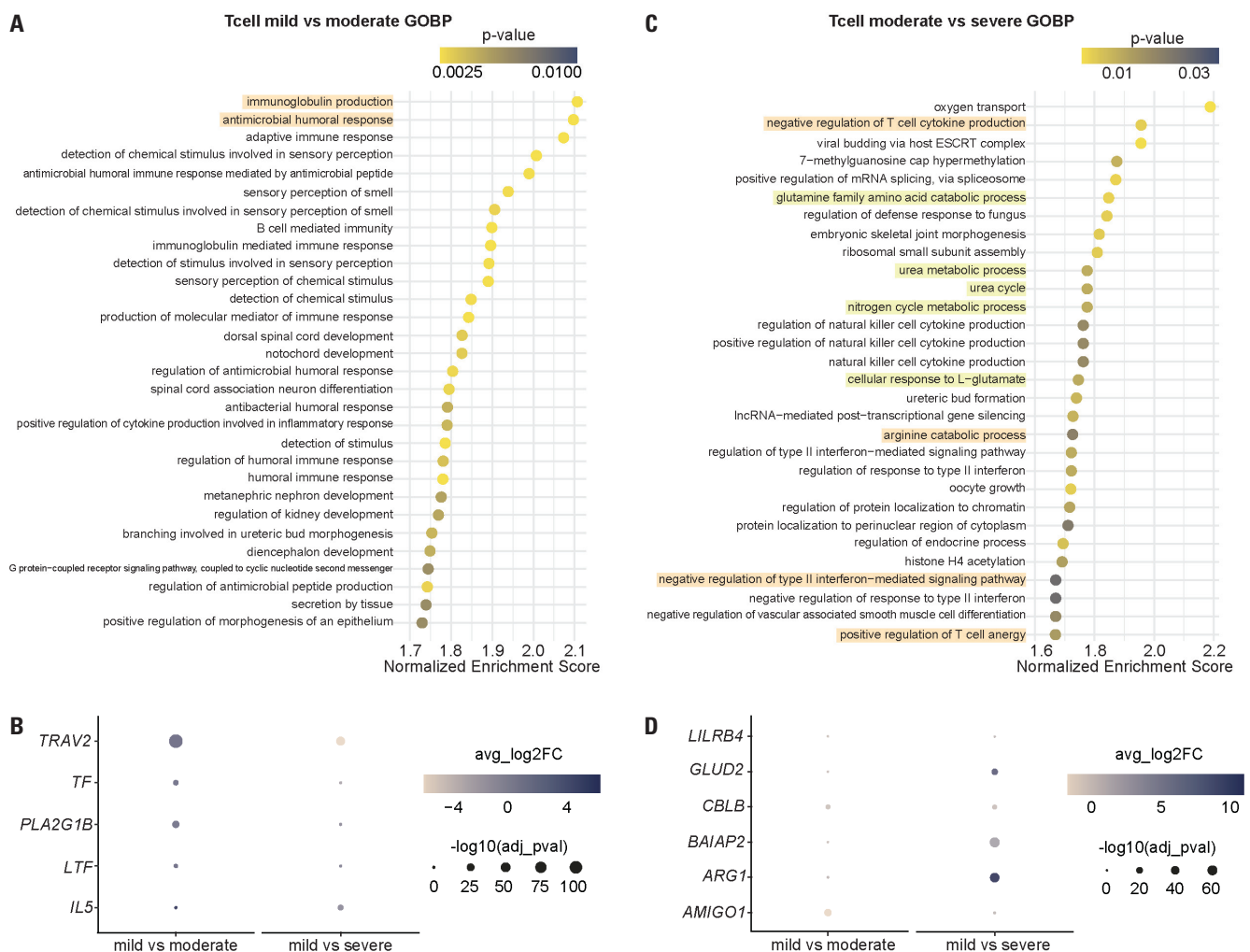


Fig. 4. Distinct pathway trends in T cells emerge as COPD advances. (A) Dot plot depicts the outcomes of GSEA based on GOBP in T cells of mild and moderate patients. The plot presents NES in descending order along with significant p -values. Notably, pathways primarily related to immune response are prominently represented at the top, highlighted with a red box. (B) Dot plots illustrate the average log2 fold change and -log10 adjusted p -values of top genes associated with high pathways identified in (A). The values were calculated during the identification of DEGs. Similarly to the top genes associated with increased pathways in moderate, they exhibit the most robust expression levels in moderate. (C) Dot plot represents the result of GSEA based on GOBP, comparing T cells from moderate and severe patients. In contrast to the findings in (A), pathways associated with decreased immune response in severe are observed to decrease, while pathways related to fibrosis show an increase. Pathways highlighted with a red box indicate those linked to decreased immune response, and pathways highlighted with a yellow box are related to fibrosis. (D) Dot plot displays the average log2 fold change and -log10 adjusted p -values of top genes related to pathways identified as significant in (C). The values were derived during the calculation of DEGs. Similarly, they also confirm the highest expression levels in severe patients. COPD, chronic obstructive pulmonary disease; GSEA, Gene Set Enrichment Analysis; GOBP, Gene Ontology Biological Processes; NES, normalized enrichment score; avg_log2FC, average log2 fold change; -log10 (adj_pval), -log10 adjusted p -value.

justed *p*-values for DEGs between MM, as well as between mild and severe stages. The presented genes predominantly showed an increase in the moderate stage and a decrease in the severe stage. This indicates a congruence in trends between the outcomes of GSEA analysis and gene expression profiling.

However, the pathways such as negative regulation of T cell cytokine production, positive regulation of T cell anergy, negative regulation of type II interferon-mediated signaling pathway, and arginine catabolic process were notably stronger in the severe stage, indicating a decrease in T cell activation and a reduction in immune response (Fig. 4C). Additionally, fibrosis-associated signals highlighted in yellow, such as glutamine family amino acid catabolic process, urea metabolic process, urea cycle, nitrogen cycle metabolic process, and cellular response to L-glutamate, were observed in the severe stage. When comparing the average expression levels of genes showing high ranks in these pathways, including AMIGO1, ARG1, BAIAP2, CBLB, GLUD2, and LILRB4, a consistent pattern emerged; they were notably upregulated during the severe stage (Fig. 4D). This finding underscores the dynamic behavior of T cells concerning COPD progression, noting varying responses of T cells as COPD advances through its stages.

Comparative features of COPD and COVID-19

Similar to COPD, COVID-19 also affects the lungs through respiratory conditions. Therefore, we conducted a pathway analysis to identify trends comparable to certain phases of COPD (Fig. 5A). The ongoing analysis used COPD sc RNA-seq data alongside new data from COVID-19 patients. The COVID-19 snRNA-seq dataset comprised seven control individuals and 20 patients obtained from GSE171524 (Table 2). To explore potential differences in T cell responses in COVID-19 compared to COPD across different stages, we conducted GSEA analysis based on the Gene Ontology Biological Processes (Fig. 5B). The analysis revealed the expression of immune response-related pathways, such as positive regulation of cytokine production, activation of innate immune response, regulation of T cell mediated immunity, T cell mediated immunity, activation of immune response, positive regulation of T cell mediated immunity, innate immune response, and regulation of cytokine. Thus, the robust immune response evident in T cells of COVID-19 patients, marked by acute reactions, bore resemblance to the vigorous immune response noted in T cells of moderate COPD patients. In addition to GSEA analysis, we investigated the expression levels of genes strongly associated with immune response pathways, such as HSP90AA1, PLCG2, ERBIN, and LYST, in both COPD and COVID-19 datasets (Fig. 5C). Surprisingly, all genes exhibited significantly higher expression levels in the moderate stage of COPD, along with significant *p*-values. Similarly, these genes showed substantial differences in expression levels between COVID-19 patients and control individuals in COVID-19 dataset. This underscores the dynamic nature of T cells as COPD progresses, and suggests that COVID-19 mirrors

trends observed in the moderate stage of COPD.

DISCUSSION

Despite its high mortality rate, COPD remains one of the most prevalent disease.²¹ Within COPD, the role of T cells has been highlighted by their correlation with the severity of the disease and the extent of lymphocyte infiltration in the lungs.²² Subsequent studies have demonstrated that T cells have been shown to migrate between inflammatory lesions in the airways and regional lymph nodes.²³ Furthermore, T cells can induce tissue damage through direct cell lysis and by mobilizing and stimulating other immune cells.²⁴ Moreover, T cells in peripheral blood of COPD patients have demonstrated heightened activation and production of diverse mediators. Several of these aberrations in T cell function have shown a significant correlation with disease severity.²⁵ Recent investigations have identified an elevation of CD8⁺ TEMRA cells in the lungs of patients with mild to moderate COPD, suggesting their potential role in initiating inflammation prior to the manifestation of severe disease.²⁶ These prior investigations provide further evidence supporting the significant role of T cells in COPD.

However, there is currently a paucity of research focused on identifying targets for tailored therapies based on the distinct stages of COPD. While there have been previous studies leveraging gene expression analyses, there is currently limited activity in the specific domain of scRNA analysis.²⁷ Therefore, we aimed to explore how T cells should be approached differently based on the stage of COPD by conducting scRNA analysis on lung tissues from COPD patients. We examined the variations in T cells across different stages of COPD and explored the resulting implications. Remarkably, transitioning from mild to moderate stages was marked by a pronounced increase in immune response. Unexpectedly, as COPD progressed from moderate to severe stages, there was a decrease in immune response coupled with a simultaneous increase in phenomena associated with fibrosis. Our findings indicated that T cells exhibited dynamic behavior and displayed distinct responses as COPD advanced.

Our findings indicate that the observed dynamic responsiveness of T cells as COPD advances suggests the potential for exploring alternative treatments tailored to this phenomenon. Understanding the intricate activation of T cells and identifying alternative therapeutic targets aligned with this understanding could lead to more effective treatment outcomes. The current treatment guidelines for COPD recommend a stepwise approach based on severity.²⁸ In stage 0, influenza vaccination is advised to mitigate risk factors. Vaccination has been shown to reduce severe symptoms and mortality rates by approximately 50% in COPD patients, particularly among the elderly. From stage 1, also known as mild, the use of bronchodilators is recommended. From stage 2, also known as moderate, regular

treatment with one or more long-acting bronchodilators, along with pulmonary rehabilitation, is encouraged. In stage 3, the addition of corticosteroids is recommended, and in stage 4,

consideration is given to long-term oxygen therapy and surgical interventions in cases of chronic respiratory failure. Additionally, antibiotic therapy, mucolytics, antioxidants, immuno-

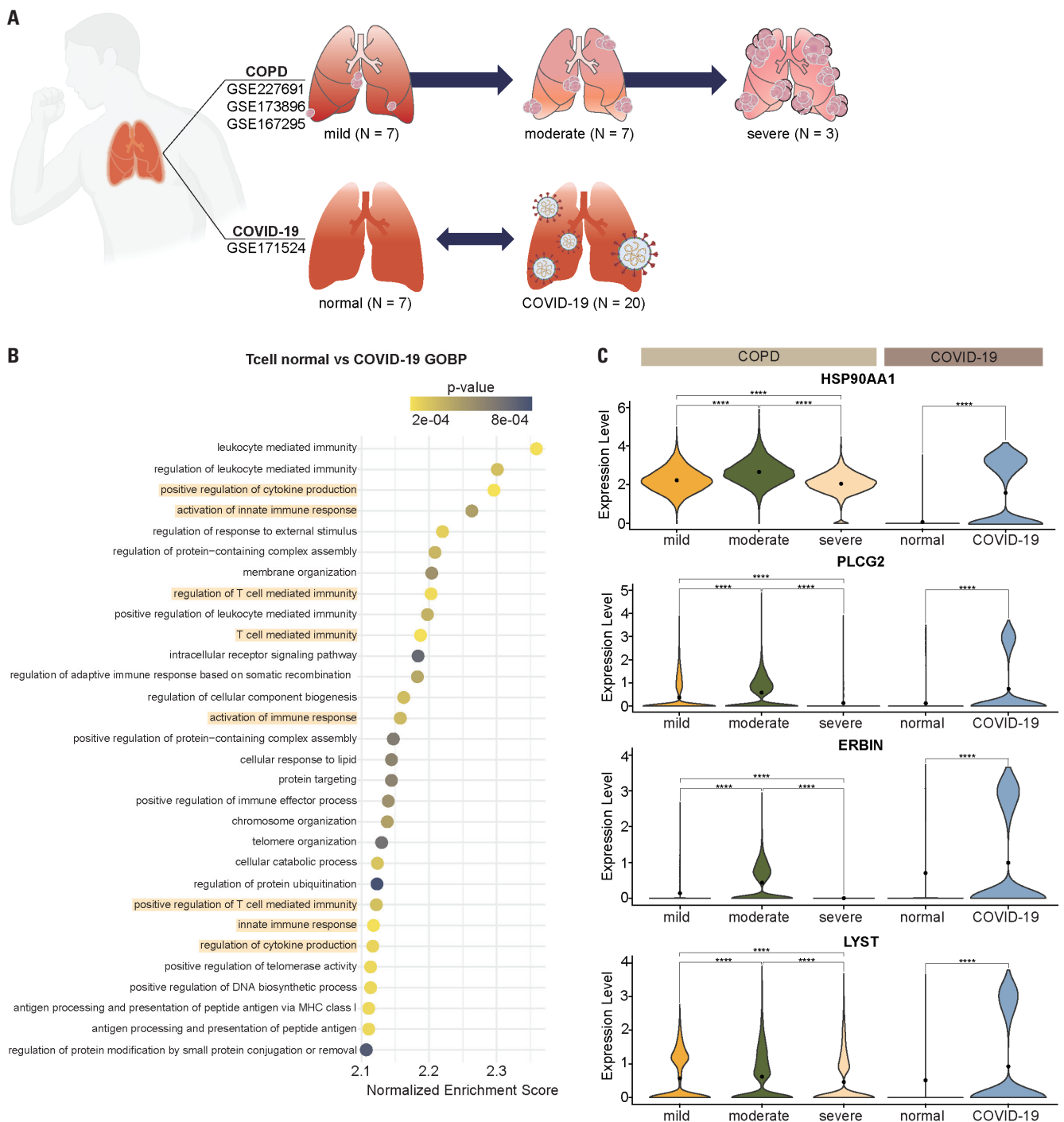


Fig. 5. Similar traits between moderate COPD and COVID-19. (A) Overview of analysis conducted using COVID-19 patient data. The COPD patient data remained consistent throughout, while the COVID-19 patient data was obtained from GSE171524, comprising seven control individuals and 20 COVID-19 patients. (B) Dot plot shows the GSEA results comparing COVID-19 patients and control individuals. Many pathways related to immune response were prominently identified in the top 30. Pathways highlighted with an orange box denote those associated with immune response. When compared to Fig. 4, similar trends are observed in the GSEA results of COPD moderate patients. (C) Violin plots illustrate the expression levels of top genes associated with immune-response related pathways significantly observed in (B). In COPD data, the highest expression is noted in moderate patient, while COVID-19 patients show a notable different expression compared to control individuals (**** $p < 0.0001$). COPD, chronic obstructive pulmonary disease; GOBP, Gene Ontology Biological Processes; GSEA, Gene Set Enrichment Analysis.

modulators, mucoregulators, respiratory stimulants, and analgesics are suggested for pharmacological treatment. However, current therapeutic paradigms primarily focus on symptom management. Alongside symptom-focused treatment, considering the diverse responses of pulmonary T cells may lead to the development of tailored therapeutic strategies for each stage.

The global outbreak of COVID-19 in 2019 was triggered by the emergence of SARS-CoV-2.²⁹ The virus exhibited a remarkably high level of contagion, resulting in a spectrum of outcomes ranging from mild illness to severe systemic inflammation, acute respiratory distress syndrome, and pneumonia in more severe cases.^{30,31} Many studies have explored the association between COVID-19 and COPD. They have noted similarities in symptoms and highlighted the potential for COVID-19 to exacerbate outcomes, including compromised lung function, particularly among COPD patients.³¹⁻³³ Consequently, the vulnerability to viral infections such as SARS-CoV-2 has been recognized in COPD patients, prompting extensive collaborative research efforts. Our study also observed patterns similar to those observed in moderate cases when examining disease concurrently. This suggests that with further robust research, treatments for COPD and COVID-19 may potentially complement each other in managing these conditions.

Based on these characteristics, more vigorous research efforts are warranted for the effective treatment of COPD in the future. Further research should not be limited to T cells but should extend to other cell types, investigating differences across stages of COPD comprehensively. Furthermore, it is imperative to explore diseases such as asthma that exhibit similar trends to COPD, in addition to COVID-19.

DATA AVAILABILITY STATEMENT

The bulk RNA sequencing data were derived from datasets available on the Gene Expression Omnibus, specifically GSE162154 and GSE239897. Additionally, single-cell RNA sequencing employed datasets GSE227691, GSE173896, and GSE167295. COVID-19 single-nuclei RNA sequencing data were derived from GSE171524.

ACKNOWLEDGEMENTS

This work was supported by the National Research Foundation of Korea (NRF-2021R1A2C2009749) and the Ministry of Health and Welfare (HR18C001202) to S.F.

AUTHOR CONTRIBUTIONS

Conceptualization: Sungsoo Fang. **Data curation:** Chae Min Lee and Andrew Sehoon Kim. **Formal analysis:** Chae Min Lee and Andrew Sehoon Kim. **Funding acquisition:** Sungsoo Fang. **Investigation:** Chae Min Lee and Andrew Sehoon Kim. **Methodology:** Chae Min Lee and Andrew Sehoon Kim. **Project administration:** Sungsoo Fang.

Resources: Chae Min Lee and Andrew Sehoon Kim. **Software:** Chae Min Lee, Andrew Sehoon Kim, and Nahee Hwang. **Supervision:** Sungsoo Fang, Minki Kim, Jae Woong Jeong, and Sugyeong Jo. **Validation:** Chae Min Lee and Andrew Sehoon Kim. **Visualization:** Chae Min Lee. **Writing—original draft:** Chae Min Lee and Andrew Sehoon Kim. **Writing—review & editing:** Chae Min Lee and Andrew Sehoon Kim. **Approval of final manuscript:** all authors.

ORCID iDs

Chae Min Lee	https://orcid.org/0009-0008-7290-4304
Andrew Sehoon Kim	https://orcid.org/0009-0008-5690-5243
Minki Kim	https://orcid.org/0000-0002-5587-9935
Jae Woong Jeong	https://orcid.org/0000-0003-4740-3467
Sugyeong Jo	https://orcid.org/0009-0005-5484-9506
Nahee Hwang	https://orcid.org/0009-0008-3895-3225
Sungsoo Fang	https://orcid.org/0000-0003-0201-5567

REFERENCES

- Li X, Cao X, Guo M, Xie M, Liu X. Trends and risk factors of mortality and disability adjusted life years for chronic respiratory diseases from 1990 to 2017: systematic analysis for the global burden of disease study 2017. *BMJ* 2020;368:m234.
- Cho WK, Lee CG, Kim LK. COPD as a disease of immunosenescence. *Yonsei Med J* 2019;60:407-13.
- Seo JY, Hwang YI, Mun SY, Kim JH, Kim JH, Park SH, et al. Awareness of COPD in a high risk Korean population. *Yonsei Med J* 2015;56:362-7.
- Li HY, Gao TY, Fang W, Xian-Yu CY, Deng NJ, Zhang C, et al. Global, regional and national burden of chronic obstructive pulmonary disease over a 30-year period: estimates from the 1990 to 2019 global burden of disease study. *Respirology* 2023;28:29-36.
- Melms JC, Biermann J, Huang H, Wang Y, Nair A, Tagore S, et al. A molecular single-cell lung atlas of lethal COVID-19. *Nature* 2021;595:114-9.
- Gilowska I. [CXCL8 (interleukin 8)--the key inflammatory mediator in chronic obstructive pulmonary disease?]. *Postepy Hig Med Dosw (Online)* 2014;68:842-50. Polish
- Hirano T. IL-6 in inflammation, autoimmunity and cancer. *Int Immunol* 2021;33:127-48.
- Siegel JP. Effects of interferon-gamma on the activation of human T lymphocytes. *Cell Immunol* 1988;111:461-72.
- Tewary P, Yang D, de la Rosa G, Li Y, Finn MW, Krensky AM, et al. Granulysin activates antigen-presenting cells through TLR4 and acts as an immune alarmin. *Blood* 2010;116:3465-74.
- Li Y, Yang Y, Guo T, Weng C, Yang Y, Wang Z, et al. Heme oxygenase-1 determines the cell fate of ferroptotic death of alveolar macrophages in COPD. *Front Immunol* 2023;14:1162087.
- Garcillán B, Fuentes P, Marin AV, Megino RF, Chacon-Arguedas D, Mazariegos MS, et al. CD3G or CD3D knockdown in mature, but not immature, T lymphocytes similarly cripples the human TCRαβ complex. *Front Cell Dev Biol* 2021;9:608490.
- Tremble LF, McCabe M, Walker SP, McCarthy S, Tynan RF, Beecher S, et al. Differential association of CD68+ and CD163+ macrophages with macrophage enzymes, whole tumour gene expression and overall survival in advanced melanoma. *Br J Cancer* 2020;123:1553-61.
- Delisser HM, Baldwin HS, Albelda SM. Platelet endothelial cell adhesion molecule 1 (PECAM-1/CD31): a multifunctional vascular cell adhesion molecule. *Trends Cardiovasc Med* 1997;7:203-10.
- Galvagni F, Nardi F, Maida M, Bernardini G, Vannuccini S, Petra-

- glia F, et al. CD93 and dystroglycan cooperation in human endothelial cell adhesion and migration. *OncoTarget* 2016;7:10090-103.
15. Wang Y, Tang Z, Huang H, Li J, Wang Z, Yu Y, et al. Pulmonary alveolar type I cell population consists of two distinct subtypes that differ in cell fate. *Proc Natl Acad Sci U S A* 2018;115:2407-12.
 16. Sun YL, Hurley K, Villacorta-Martin C, Huang J, Hinds A, Gopalan K, et al. Heterogeneity in human induced pluripotent stem cell-derived alveolar epithelial type II cells revealed with ABCA3/SFT-PC reporters. *Am J Respir Cell Mol Biol* 2021;65:442-60.
 17. Endale M, Ahlfeld S, Bao E, Chen X, Green J, Bess Z, et al. Temporal, spatial, and phenotypical changes of PDGFR α expressing fibroblasts during late lung development. *Dev Biol* 2017;425:161-75.
 18. Higham A, Dungwa J, Pham TH, McCrae C, Singh D. Increased mast cell activation in eosinophilic chronic obstructive pulmonary disease. *Clin Transl Immunology* 2022;11:e1417.
 19. Zhang DW, Ye JJ, Sun Y, Ji S, Kang JY, Wei YY, et al. CD19 and POU2AF1 are potential immune-related biomarkers involved in the emphysema of COPD: on multiple microarray analysis. *J Inflamm Res* 2022;15:2491-507.
 20. Franzén O, Gan LM, Björkegren JLM. PanglaoDB: a web server for exploration of mouse and human single-cell RNA sequencing data. *Database (Oxford)* 2019;2019:baz046.
 21. Barnes PJ, Burney PG, Silverman EK, Celli BR, Vestbo J, Wedzicha JA, et al. Chronic obstructive pulmonary disease. *Nat Rev Dis Primers* 2015;1:15076.
 22. Finkelstein R, Fraser RS, Ghezzi H, Cosio MG. Alveolar inflammation and its relation to emphysema in smokers. *Am J Respir Crit Care Med* 1995;152(5 Pt 1):1666-72.
 23. Lehmann C, Wilkening A, Leiber D, Markus A, Krug N, Pabst R, et al. Lymphocytes in the bronchoalveolar space reenter the lung tissue by means of the alveolar epithelium, migrate to regional lymph nodes, and subsequently rejoin the systemic immune system. *Anat Rec* 2001;264:229-36.
 24. Monaco C, Andreaskos E, Kiriakidis S, Feldmann M, Paleolog E. T-cell-mediated signalling in immune, inflammatory and angiogenic processes: the cascade of events leading to inflammatory diseases. *Curr Drug Targets Inflamm Allergy* 2004;3:35-42.
 25. Gadgil A, Zhu X, Sciurba FC, Duncan SR. Altered T-cell phenotypes in chronic obstructive pulmonary disease. *Proc Am Thorac Soc* 2006;3:487-8.
 26. Villaseñor-Altamirano AB, Jain D, Jeong Y, Menon JA, Kamiya M, Haider H, et al. Activation of CD8+ T cells in chronic obstructive pulmonary disease lung. *Am J Respir Crit Care Med* 2023;208:1177-95.
 27. Chen ZH, Kim HP, Ryter SW, Choi AM. Identifying targets for COPD treatment through gene expression analyses. *Int J Chron Obstruct Pulmon Dis* 2008;3:359-70.
 28. Agustí A, Celli BR, Criner GJ, Halpin D, Anzueto A, Barnes P, et al. Global initiative for chronic obstructive lung disease 2023 report: GOLD executive summary. *Eur Respir J* 2023;61:2300239.
 29. Coronaviridae Study Group of the International Committee on Taxonomy of Viruses. The species severe acute respiratory syndrome-related coronavirus: classifying 2019-nCoV and naming it SARS-CoV-2. *Nat Microbiol* 2020;5:536-44.
 30. Puhach O, Meyer B, Eckerle I. SARS-CoV-2 viral load and shedding kinetics. *Nat Rev Microbiol* 2023;21:147-61.
 31. Hu B, Guo H, Zhou P, Shi ZL. Characteristics of SARS-CoV-2 and COVID-19. *Nat Rev Microbiol* 2021;19:141-54.
 32. Rajabi H, Mortazavi D, Konyalilar N, Aksoy GT, Erkan S, Korkunc SK, et al. Forthcoming complications in recovered COVID-19 patients with COPD and asthma; possible therapeutic opportunities. *Cell Commun Signal* 2022;20:173.
 33. Awatade NT, Wark PAB, Chan ASL, Mamun SMAA, Mohd Esa NY, Matsunaga K, et al. The complex association between COPD and COVID-19. *J Clin Med* 2023;12:3791.